Frequency Filtering in Telecommunications

Ariadna Farres Basiana
Universitat Autonoma de Barcelona, Spain
e-mail: `ariminus@hotmail.com`

Hanna Martinsson
Chalmers University of Technology, Sweden
e-mail: `hannam@math.chalmers.se`

Brage Ofstad Vik
Norwegian University of Science and Technology, Norway
e-mail: `brageofs@stud.math.ntnu.no`

Sergiy Pereverzyev
University of Kaiserslautern, Germany
e-mail: `pereverz@mathematik.uni-kl.de`

Martin Purrucker
Chemnitz University of Technology, Germany
e-mail: `mapu@mathematik.tu-chemnitz.de`

Klaus Erich Schmitz Abe
University of Oxford, UK
e-mail: `schmitz@maths.ox.ac.uk`

David Stiel
Technical University of Denmark, Denmark
e-mail: `c973794@student.dtu.dk`

Uldis Strautins
University of Kaiserslautern, Germany
e-mail: `strauti@mathematik.uni-kl.de`

*This document was prepared for the Proceedings of the **17-th ECMI Modelling Week** which was held from 22.08.2003 till 31.08.2003 in Bristol, UK. The problem was proposed by Sabine Zaglmayr* who also made supervision of the group.*

Abstract

Piezoelectric filters are used in telecommunication to filter electrical signals. This report deals with the problem of calculating passing and damped frequency intervals for a filter with given geometrical configurations and materials. Only periodic filters, which are widely used in practice, were considered. These filters consist of periodically arranged cells. For a small amount of cells a numerical procedure to visualise the wave propagation in the filter was developed. For a big number of cells another model of the filter was obtained. In this model it is assumed that the filter occupies an infinite domain. This leads to a differential equation, with periodic coefficients, that describes propagation of the wave with a given frequency in the filter. To analyse this equation the Spectral Theory for Periodic Operators had to be employed. Different ways – analytical and numerical – to apply the theory were proposed and analysed.

* *Johannes Kepler University Linz, Austria*; **e-mail:** `sz@jku.at`

Acknowledgements

First of all, we would like to thank Dr. Eddie Wilson for the organisation of the Modelling Week and for the great time we all had in Bristol. We also express our gratitude to our instructor Sabine Zaglmayr for this both exciting and interesting problem, for her readiness to discuss occurring difficulties, for hours of inspiring discussions and for her numerous corrections and ideas on this report.

Sergiy Pereverzyev and Uldis Strautins would like to thank Dr. Falk Triebsch for giving the chance to participate in the Modelling Week and handling all formalities. David Stiel would like to send his gratitude to Mads Peter Sørensen for the exact same reasons. Klaus Schmitz would like to say thanks to Dr. Hilary Ockendon for all her help and confidence in him.

Contents

1 Introduction

1.1 Problem description

As telecommunication is getting more and more widespread, the quantity of electromagnetic waves surrounding us is increasing rapidly. Some of the devices sending and/or receiving such waves are TV's, radios, satellite dishes, mobile phones and more recently wireless computer networks. In order for these devices to function properly, it is necessary for them to filter out any unwanted information, wherefore a variety of filters (that only allows certain frequencies to pass through) have been developed. We have studied the so-called periodic *Surface Acoustic Wave* (SAW) filters which are widely used in practice.

A SAW filter consists of a piezoelectric material and a sender and receiver comb of large number of electrodes (>1000). The electrodes in each comb are periodically distributed on the top of the piezoelectric material. A schematic representation of the 2D cut along the SAW filter is presented in Figure 1.

Figure 1: 2D cut along the SAW filter.

A piezoelectric material generates an electric field (voltage) when it is submerged to mechanical forces (or stresses), and, alternatively, produces a mechanical force (or displacement) when a voltage is applied. These effects are respectively called the *direct* and *inverse piezoelectric effects.*

Let us briefly describe how the filter works in a mobile phone or a similar device. An incoming electromagnetic wave is received by the antenna and transformed into an electric signal. It is this electric signal we whish to filter. The electric signal is applied on the input electrodes. Due to the direct piezoelectric effect a mechanical wave is produced on the surface. The wave will travel along the surface. When the mechanical wave reaches the output end, due to the inverse piezoelectric effect one can measure an electric field on the output electrodes.

While the waves travel through the filter, some frequencies are damped and thus will be missing in the output signal. "An engineer's explanation" for this phenomena is the following: during the wave propagation inside the filter, a small wave reflection occurs at each electrode. If the reflected waves sum up constructively (Figure 2a) the result will be a wave which moves in the opposite direction to the traveling wave. This causes damping. Otherwise, if the reflections cancel each other (Figure 2b), the traveling wave will propagate through the filter without damping.

Whether reflections sum up constructively or not depends on the relationship between the frequency of the traveling wave and the materials and the arrangement of the electrodes in the filter. Knowing these parameters (materials and arrangement) we whish to split the frequency domain into passing and damped regions. An outline of our work follows.

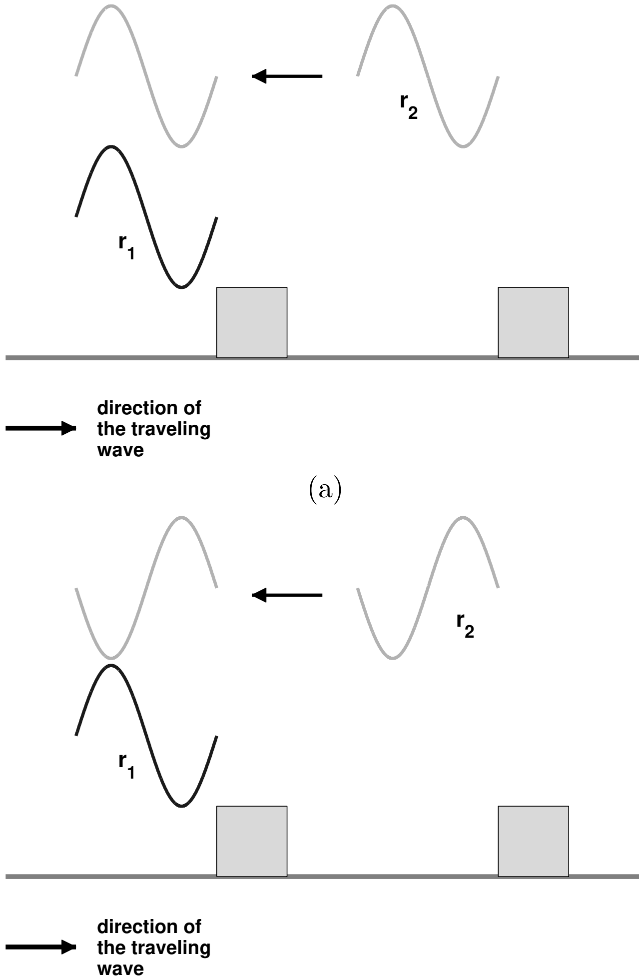

(b)

Figure 2: Illustration of the damping phenomena: (a) — The reflected waves from the electrodes r_1 and r_2 sum up constructively and thus damp the traveling wave; (b) — The reflected waves cancel each other and therefore do not affect the traveling wave.

1.2 Organization of the report

In **Section 2** we start by modeling the filter geometry. Then the full system of differential equations that governs the wave propagation in a piezoelectric filter is presented. This system is simplified to the well known wave equation in 1D. For a small amount of electrodes a numerical procedure to visualize the wave propagation in the filter is developed. The numerical results hereof, which show the damping phenomena, are presented. Since in many practical applications the number of electrodes is huge, the model of the filter occupying an infinite domain is obtained and analyzed in **Section 3**.

By a shift from the time to the frequency domain we obtain a differential equation with periodic coefficients, that describes propagation of the wave with a given frequency. To analyse this equation we state and prove the *Bloch-Floquet Theorem* for abstract periodic operators. The theorem enables us to make predictions on the behaviour of waves with given frequencies in the whole (infinite) domain from their behaviour in a single cell. Two different ways to apply the theory, analytical and numerical, are proposed in **Sections 4** and **5** respectively. In these sections passing and damped frequency intervals are calculated. Finally in **Section 6** we present a summary and outlook for future research.

2 Filter Model: *Bounded Domain Considerations*

2.1 Model for the filter geometry

Before stating the governing equations for the filter, let us consider the domain on which the equations will be defined. The domain can be described so that its construction reflects the periodicity of the material properties, thus inheriting some fundamental properties of the filter.

The filter consists of n equal equidistant electrodes evaporated on a piezoelectric surface, where n may reach several thousands. Such a domain can be described as a union of congruent unit cells. We will assume that the (unperturbed) filter has a rectangular structure, and that the distance between (the centers of) neighbouring electrodes is p, see Figure 3. Define the reference element

$$\Omega(x) = [x, p + x] \times [0, q] \times [0, r] \subset \mathbb{R}^3.$$

Then the filter as a domain can be described by

$$\Omega_n = \bigcup_{j=0}^{n-1} \Omega(jp).$$

Since the material properties of the filter are p-periodic in the x-direction, it is sufficient to define them only one cell, the reference cell, say $\Omega(0)$.

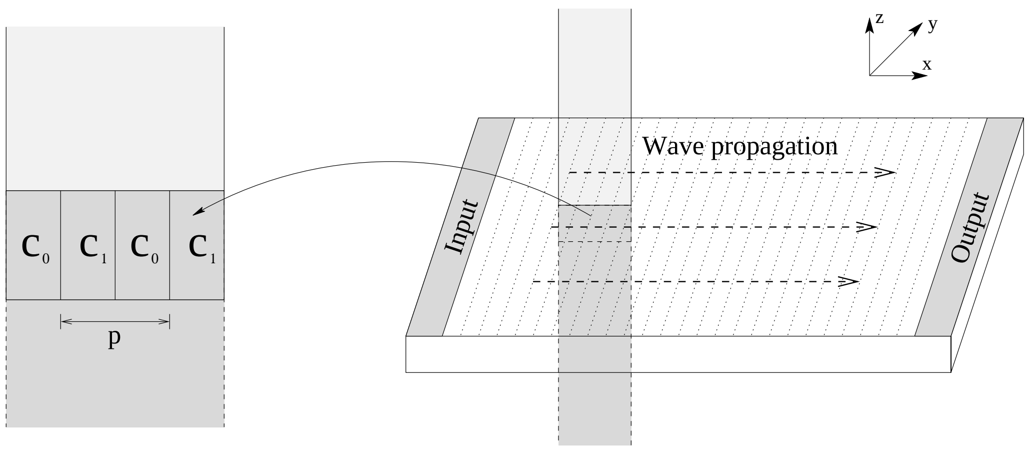

Figure 3: The model of the filter.

2.2 Governing equations

2.2.1 Piezoelectric equations

The behaviour of the filter is described through the system of piezoelectric equations (see for example [OLI, p. 14]). Let u denote the displacement vector field in the material, T - stress tensor field, E - electric field, and D - dielectric displacement field. The equations consist of:

- *Equations of motion* (Newton's law), part of Maxwell equations when there are no free charges in the material (insulated material):

$$\operatorname{div} T = \rho \frac{\partial^2 u}{\partial t^2}, \tag{1a}$$

$$\operatorname{div} D = 0. \tag{1b}$$

- Equations describing *piezoelectric material properties*, i.e. coupling of mechanical and the electric field $E = -\nabla\phi$ with potential ϕ:

$$T = \frac{c}{2}(\,(\nabla u)^\top + \nabla u\,) + e\nabla\phi, \tag{2a}$$

$$D = \frac{e^T}{2}(\,(\nabla u)^\top + \nabla u\,) - \varepsilon\nabla\phi. \tag{2b}$$

Here c is the stiffness tensor, ε - dielectric permittivity tensor, e - piezoelectric coupling tensor and ρ - mass density of the material. All of these material properties are functions of $\mathbf{x} = (x, y, z) \in \Omega_n$.

For equations (1a)-(2b) corresponding initial and boundary conditions should be specified.

This is a rather exact model of the filter. As a first simplification, we will neglect the piezoelectric coupling between (2a) and (2b). Thus, we will only consider the mechanical problem, of how a periodic change of the material properties influences wave propagation. As we shall see, the resulting equation exhibits properties of a frequency band filter.

2.2.2 Wave equation

If we neglect the coupling between mechanical stresses and electrical fields in the piezoelectric material we can insert (2a) into (1a) to get the following equation for the mechanical displacement for $\mathbf{x} \in \operatorname{int}(\Omega_n)$:

$$\operatorname{div}\left(\frac{c(\mathbf{x})}{2}(\nabla^T u(\mathbf{x}) + \nabla u(\mathbf{x}))\right) = \rho(\mathbf{x})\frac{\partial^2 u}{\partial t^2}. \tag{3}$$

We assume that density is constant in the material, i.e. $\rho(\mathbf{x}) \equiv \rho,\ \forall \mathbf{x} \in \Omega_n$. This is not a severe restriction and all presented techniques can be extended for nonconstant densities. Using this assumption, we may consider the function $\bar{c}(\mathbf{x}) = \frac{c(\mathbf{x})}{\rho}$. In the following we will omit the bar and write just $c(\mathbf{x})$. The physical interpretation of such defined function $c(\mathbf{x})$ will be presented later.

The function c needs only to be defined on a single cell, whereafter it can be extended periodically to other cells. A cell consists of the piezoelectric material and an electrode. We assume that c is constant in each of the two parts of a cell, so that

$$c(\mathbf{x}) = \begin{cases} c_0, & \text{for piezoelectric material,} \\ c_1, & \text{for electrode.} \end{cases}$$

Remark 2.1 *Note that since c is in general discontinuous (at the interface between materials), the equation (3) as well as the piezoelectric system are not defined in classical sense. But they do make sense in weak formulations. We will consider this formulation in more detail in Section 3.*

We observe that all important characteristics of the filter, e.g., the periodicity of the materials and the direction of wave propagation, are given in the direction of x. This inspires us to make an one-dimensional approximation, simplifying (3) to the following wave equation:

$$\frac{\partial}{\partial x}\left(c(x)\frac{\partial u}{\partial x}\right) = \frac{\partial^2 u}{\partial t^2}, \tag{4}$$

with coefficient (now one-dimensional), defined on one period by

$$c(x) = \begin{cases} c_0, & x \in (0,l), \\ c_1, & x \in (l,p), \end{cases} \tag{5}$$

and extended periodically by

$$c(x+p) = c(x)$$

for $x \in [0,(n-1)p]$. According to [TSM, p. 32], $\sqrt{c(x)}$ is the local speed of wave propagation in the material.

Equation (4) is valid for $t > 0$ and $x \in [0, np]$. We define $d := np$. To finish the 1D model of the filter we should specify initial and boundary conditions for (4). We suppose that initially the media in the filter is undisturbed, i.e.

$$\begin{cases} u(x,0) & = & 0 \\ \dfrac{\partial u}{\partial t}(x,0) & = & 0 \end{cases} \quad x \in [0,d]. \tag{6}$$

At one end of the filter, which we will call the *input end*, the input signal $\varphi_{\text{in}}(t)$ is applied. At the other end, called the *output end*, we will collect the output signal $\varphi_{\text{out}}(t)$. We assume that the input end corresponds to $x = 0$, and the output end to $x = d$. We will model the input signal as a Dirichlet boundary condition:

$$u(0,t) = \varphi_{\text{in}}(t), \ t > 0.$$

What kind of boundary conditions should be imposed at the output end? Neumann or mixed type boundary conditions would cause wave reflection from the output end. We want only to measure the function u at the output end, but do not want to cause any disturbance, in form of reflection, on the wave propagation. So, a special non-reflecting boundary condition should be used. We will derive it in the following subsection.

2.3 Non-reflecting boundary condition

The wave will not be reflected from the output end, if it is allowed to travel further. This is the case when behind the output end there is a homogeneous media with the propagation speed $\sqrt{c_{\text{hom}}} := \sqrt{c(d)}$ (Figure 4). Let $u_{\text{hom}}(x,t)$ denote the displacement in this material. Then u_{hom} satisfies the following wave equation

$$c_{\text{hom}}\frac{\partial^2 u_{\text{hom}}}{\partial x^2}(x,t) = \frac{\partial^2 u_{\text{hom}}}{\partial t^2}(x,t), \quad \text{for } x > d, \ t > 0 \tag{7}$$

The initial conditions will be taken as (6). Since (7) is defined for $x > d$, we need boundary conditions only in $x = d$. These boundary conditions are taken from the coupling of the solutions in the domains D_1 and D_2 (see (21a) and (21b)):

$$u_{\text{hom}}(d,t) = u(d,t) \tag{8a}$$

$$c_{\text{hom}}\frac{\partial u_{\text{hom}}}{\partial x}(d,t) = c(d)\frac{\partial u}{\partial x}(d,t). \tag{8b}$$

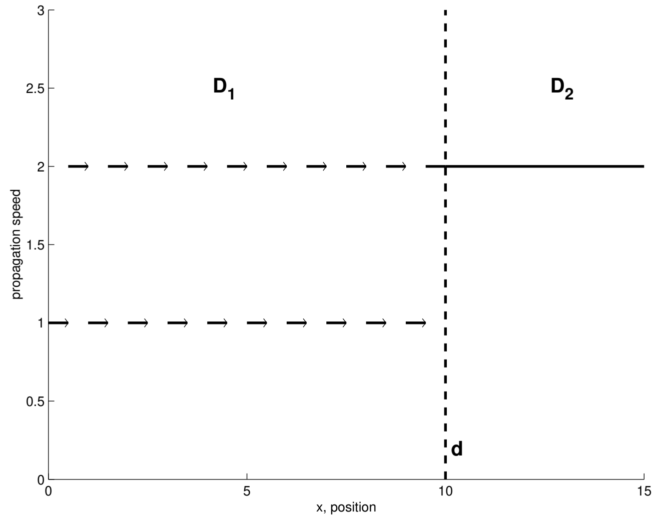

Figure 4: Propagation speed inside the filter (D_1) and in the homogeneous material (D_2) outside the output end.

It appears that equation (7) with zero initial conditions and boundary condition (8a) and (8b) can be solved analytically. As a direct consequence of [TSM, p. 66] we have

$$u_{\text{hom}}(x,t) = u\left(d, t - \frac{x-d}{\sqrt{c_{\text{hom}}}}\right), \quad x - d \le \sqrt{c_{\text{hom}}}t. \tag{9}$$

Plugging expression (9) into (8b) we obtain the desired non-reflecting boundary condition for u:

$$\frac{\partial u}{\partial x}(d,t) = -\frac{1}{\sqrt{c_{\text{hom}}}} \cdot \frac{\partial u}{\partial t}(d,t). \tag{10}$$

Now we may write the whole initial boundary value problem for u (see Remark 2.1) :

$$\begin{cases} \dfrac{\partial}{\partial x}\left(c(x)\dfrac{\partial u}{\partial x}\right) = \dfrac{\partial^2 u}{\partial t^2}, \quad x \in (0,d), \ t > 0; \\[2ex] \left.\begin{array}{rcl} u(x,0) & = & 0 \\ \dfrac{\partial u}{\partial t}(x,0) & = & 0 \end{array}\right\} x \in [0,d] \\[4ex] \left.\begin{array}{rcl} u(0,t) & = & \varphi_{\text{in}}(t) \\ \dfrac{\partial u}{\partial x}(d,t) & = & -\dfrac{1}{\sqrt{c(d)}} \cdot \dfrac{\partial u}{\partial t}(d,t) \end{array}\right\} t > 0. \end{cases} \tag{11}$$

We want to simulate the output signal $\varphi_{\text{out}}(t) = u(d,t)$ for any given input signal $\varphi_{\text{in}}(t)$. In the sequel we will derive a numerical method for solving (11) and present some numerical results.

2.4 Numerical method

We use the standard equidistant discretization of the space $[0,d]$ and time domain:

$$\begin{aligned} x_i &= (i-1) \cdot \frac{d}{N-1}, \quad i = 1,...,N \\ t_j &= (j-1) \cdot \tau, \qquad j = 1,2,..., \ \tau > 0. \end{aligned}$$

Let us denote

$$h = \frac{d}{N-1},$$
$$x_{i+1/2} = \frac{x_i + x_{i+1}}{2}, \qquad t_{j+1/2} = \frac{t_j + t_{j+1}}{2},$$
$$u_i^j = u(x_i, t_j).$$

For the discretization of the wave equation we will use finite volume ideas, i.e. we will apply the integration $\int_{t_{j-1/2}}^{t_{j+1/2}} \int_{x_{i-1/2}}^{x_{i+1/2}} dx\, dt$ to both sides of the wave equation in (11). The integrals are approximated by the mid point rule $\int_a^b f(u)du \approx f(\frac{a+b}{2}) \cdot (b-a)$. First order derivatives are approximated by the central difference approximation:

$$\left.\frac{\partial u}{\partial x}\right|_{x=x_{i+1/2}} \approx \frac{u(x_{i+1}) - u(x_i)}{h}.$$

We obtain:

$$\begin{aligned}
\int\limits_{t_{j-1/2}}^{t_{j+1/2}} \int\limits_{x_{i-1/2}}^{x_{i+1/2}} \frac{\partial}{\partial x}\left(c(x)\frac{\partial u}{\partial x}\right) dx\, dt \quad &\approx \quad \int\limits_{t_{j-1/2}}^{t_{j+1/2}} \Bigg[c(x_{i+1/2}) \cdot \frac{u(x_{i+1},t) - u(x_i,t)}{h} - \\
&\qquad\qquad c(x_{i-1/2}) \cdot \frac{u(x_i,t) - u(x_{i-1},t)}{h} \Bigg] dt \\
&\approx \quad \frac{\tau}{h}\Big[u_{i+1}^j \cdot c(x_{i+1/2}) - \\
&\qquad u_i^j \cdot (\, c(x_{i-1/2}) + c(x_{i+1/2})\,) + \\
&\qquad u_{i-1}^j \cdot c(x_{i-1/2}) \Big];
\end{aligned}$$

$$\int\limits_{t_{j-1/2}}^{t_{j+1/2}} \int\limits_{x_{i-1/2}}^{x_{i+1/2}} \frac{\partial^2 u}{\partial t^2} dx\, dt \quad \approx \quad \frac{h}{\tau}\left[u_i^{j+1} - 2\, u_i^j + u_i^{j-1} \right].$$

Thus for $i = 2, ..., N-1;\ j \geq 3$ we have

$$\begin{aligned}
u_i^{j+1} \quad = \quad & \left[\tfrac{\tau^2}{h^2} \cdot c(x_{i+1/2})\right] \mathbf{u_{i+1}^j} + \\
& \left[2 - \tfrac{\tau^2}{h^2} \cdot \left(\, c(x_{i+1/2}) + c(x_{i-1/2})\,\right)\right] \mathbf{u_i^j} + \\
& \left[\tfrac{\tau^2}{h^2} \cdot c(x_{i-1/2})\right] \mathbf{u_{i-1}^j} - u_i^{j-1}
\end{aligned} \tag{12}$$

Two more equations are derived from the boundary conditions:

- The Dirichlet boundary condition gives

$$u_1^{j+1} = \varphi_{\text{in}}(t_{j+1}). \tag{13}$$

- After discretization of the non-reflecting boundary condition (10) by

$$\frac{u_N^j - u_{N-1}^j}{h} = -\frac{1}{\sqrt{c(l)}} \cdot \frac{u_N^{j+1} - u_N^j}{\tau}$$

we get

$$u_N^{j+1} = \left[1 - \frac{\tau}{h}\sqrt{c(l)}\right] \mathbf{u_N^j} + \left[\frac{\tau}{h}\sqrt{c(l)}\right] \mathbf{u_{N-1}^j}. \tag{14}$$

Let us define $u^j = (u_1^j, u_2^j, ..., u_N^j)^T$. By combining equations (12), (13) and (14), we get:

$$u^{j+1} = A\,u^j + B\,u^{j-1} + v, \quad j = 2, 3, ... \tag{15}$$

where A, B are some matrices and v is a fixed vector. The vectors u^1 and u^2 are obtained from the initial conditions:

$$\begin{aligned} u^1 &= \overrightarrow{0} \\ u^2 &= (\varphi_{\text{in}}(t_2), 0, ..., 0)^T. \end{aligned}$$

To ensure stability of the scheme (15) we take

$$\tau = \frac{h}{2 \cdot \max\limits_{x \in [0,d]} \sqrt{c(x)}}, \tag{16}$$

(see for example [AMS, p. 194]).

2.5 Numerical results

We demonstrate the proposed numerical method for $n = 10$ cells. Function c is chosen as in Figure 4 (domain D_1).The number of discrete points in the space domain $[0, d]$ is chosen to $N = 150$, and the time step is chosen according to (16). All used physical variables (speed $\sqrt{c}$, displacement u, length x, time t) are scaled and do not have dimensions. We will use the harmonic input functions $\varphi_{\text{in}}(t)$ of the form:

$$\varphi_{\text{in}}(t) = A\,\sin \omega t. \tag{17}$$

Our first example is a passing signal. We take $\varphi_{\text{in}}(t) = 2 \sin\, t$. The numerical solution of (11) at different times is shown in Figure 5. One observes that the harmonic shape of the input signal is curved by the inhomogeneous media. The signal is passing through, which is clearly seen in Figure 6, where input and output signals are shown together. The filter almost does not change the amplitude and the frequency of the input signal.

In the second example we get a damped wave propagation for the input signal $\varphi_{\text{in}}(t) = 2 \sin \frac{7}{2} t$. Numerical results at different times are presented in Figure 7. One observes that for this input signal reflections from different electrodes sum up constructively, and therefore the reflected waves are concentrated at the beginning and damp the input wave. As it is seen from Figure 8, only small values of u could be measured at the output end.

These two examples show, that, depending on the frequency, there are signals which are damped and signals which can pass nearly undamped through the filter. Thus, the proposed mathematical model and the corresponding numerical method confirms "an engineer's explanation" about damping presented in the Introduction – and provides a good illustration for it.

To determine which frequencies are damped and which are not, we should run the simulations for input signals of the form (17) with different frequencies ω. As it was mentioned earlier, real filters consist of a huge amount of cells which makes numerical simulations extremely difficult: we need a lot of time and memory to run them. Hence we cannot directly apply the proposed technique to obtain passing and damped frequency intervals. Further modeling steps and analysis are required. These are presented in the following sections.

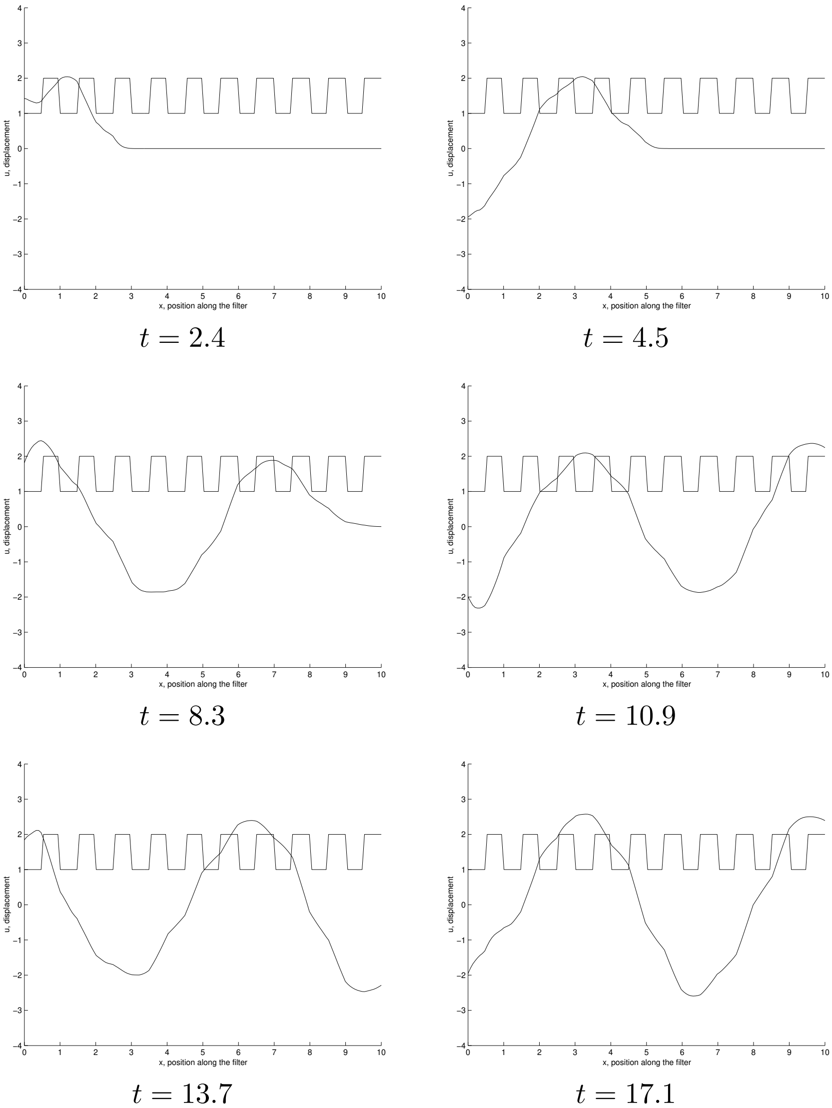

Figure 5: Results for the passing signal, $\varphi_{\text{in}}(t) = 2 \cdot \sin t$.

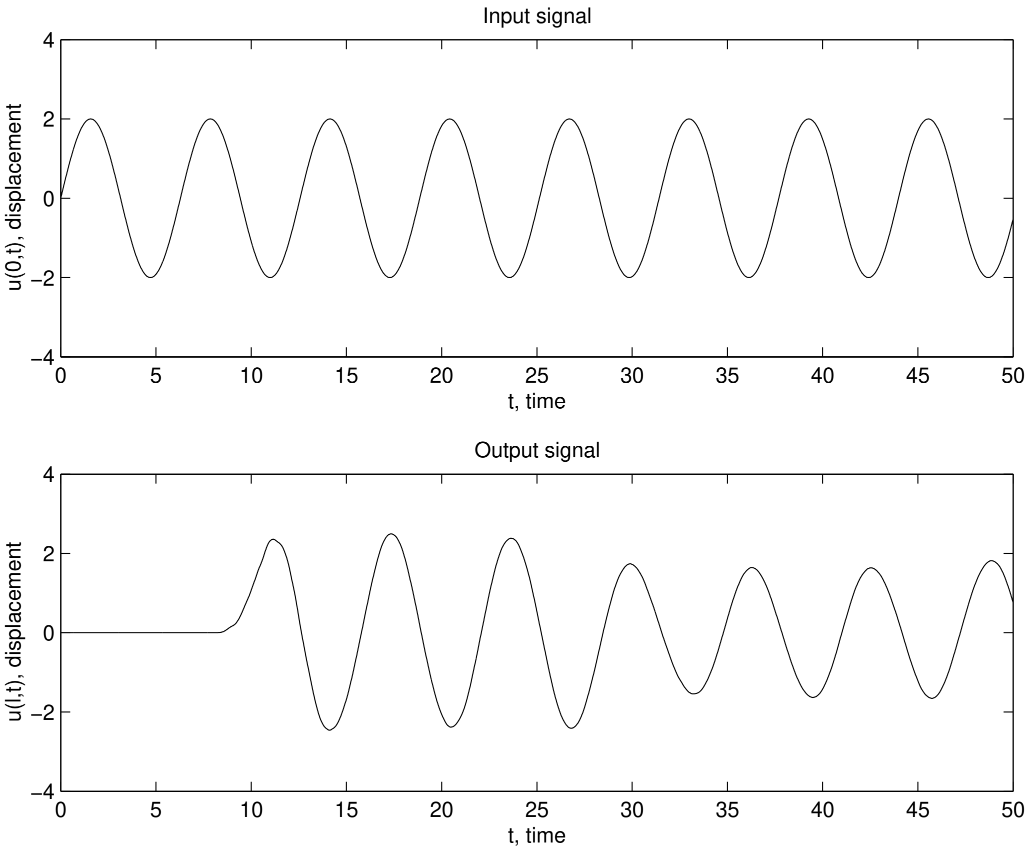

Figure 6: Input and output signals: example of a passing signal.

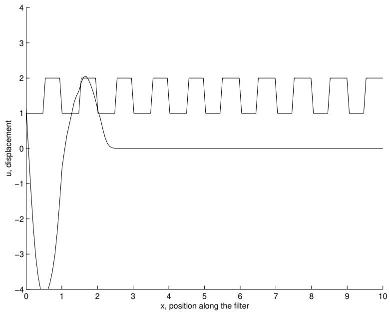

$t = 2$

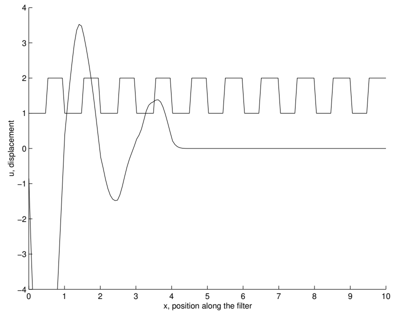

$t = 3.5$

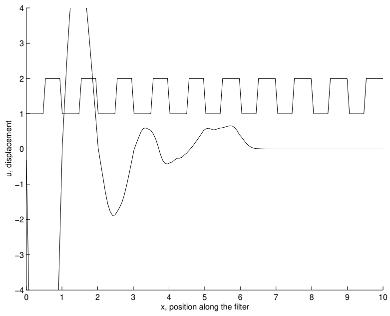

$t = 5.4$

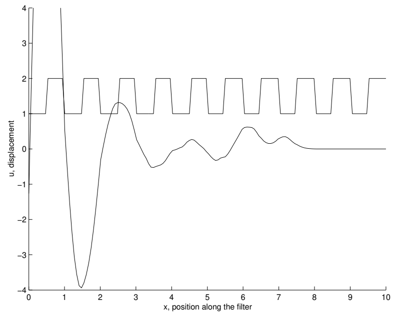

$t = 6.5$

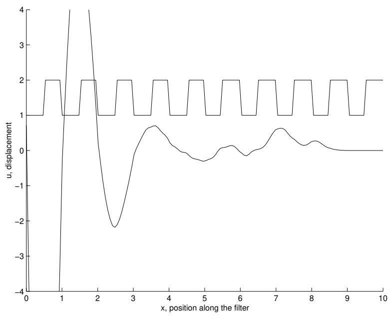

$t = 7.3$

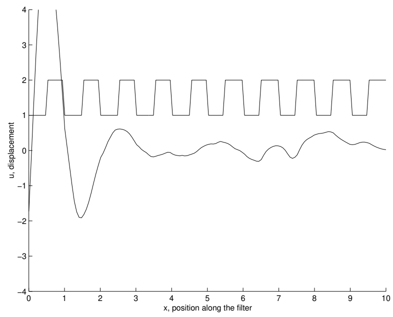

$t = 8.4$

Figure 7: Results for the damped signal $\varphi_{\text{in}}(t) = 2 \cdot \sin \frac{7}{2} t$.

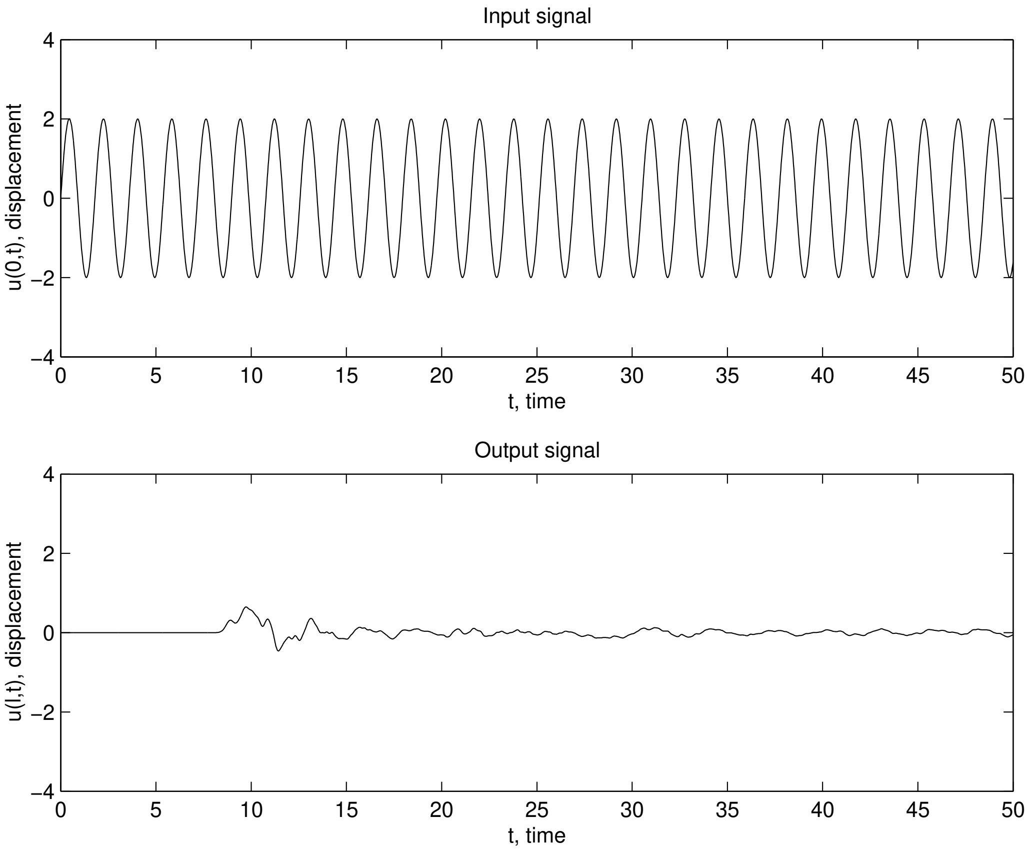

Figure 8: Input and output signals: example of a damped signal.

3 Filter Model: *Unbounded Domain Considerations*

First of all, let us note that equation (4) describes changes of the function $u(x,\cdot)$ in time. But we are actually interested in how the *spectrum* (collection of the frequencies presented in a signal/function) of the function $u(\cdot,t)$ changes in space. That is why, we will perform a shift from the **time domain** to the **frequency domain** (see e.g. [MCL, Lecture 2B]). Mathematically this is done via the inverse Fourier transform:

$$u(x,t) = \frac{1}{2\pi}\int_{-\infty}^{+\infty} \hat{u}(x,\omega)\, e^{i\omega t} d\omega. \tag{18}$$

Plugging (18) into (4) we get:

$$\int_{-\infty}^{+\infty} \left[\frac{\partial}{\partial x}\left(c(x)\frac{\partial}{\partial x}\hat{u}(x,\omega)\right) + \omega^2 \hat{u}(x,\omega)\right] e^{i\omega t} d\omega = 0.$$

Since the Fourier transform is injective and linear we may write:

$$\frac{\partial}{\partial x}\left(c(x)\frac{\partial}{\partial x}\hat{u}(x,\omega)\right) + \omega^2 \hat{u}(x,\omega) = 0. \tag{19}$$

We will skip the hat and will not write the dependency on ω explicitly. Thus (19) becomes

$$\frac{d}{dx}\left(c(x)\frac{d}{dx}u(x)\right) + \omega^2 u(x) = 0. \tag{20}$$

The next step concerns the space domain where (20) is valid. Since the number of cells is very big, we will assume that equation (20) is valid in the whole real line, $x \in \mathbb{R}$. In this case (20) is a differential equation with periodic coefficients. The behaviour of a solution to this equation in $\mathbb{R}$ can be determined from their behaviour in a single cell, eg. $[0,p]$. This is done by employing spectral properties of periodic operators. Usually it is applied to differential equations with smooth periodic coefficients. Since we do not have smooth coefficients the classical theory will have to be adapted. Before doing this we will derive a weak form of (20).

3.1 Weak interpretation

In the classical theory of differential equations, the concept of classical solution is often used. By definition, a classical solution of a k-th order differential equation must be k times continuously differentiable. However, it is easily seen that equation (20) has no classical solutions apart from constant ones, $u = 0$, if $c(x)$ is not continuously differentiable. Therefore we need to weaken the concept of solutions for this equation.

Let us assume that $c : \mathbb{R} \to \mathbb{R}$ is piecewise continuously differentiable, but not necessary continuous, i.e. $c \in C^1(\mathbb{R} \setminus G)$ where G is a finite or countable set with no accumulation points. Assume further that $c'(x)$ is bounded in $\mathbb{R} \setminus G$. Note that the function defined by (5) satisfies this conditions.

The idea is to interpret the derivatives in (20) as week derivatives rather than strong (classical) ones. A locally integrable function $Du : \mathbb{R} \to \mathbb{C}$ is called the *weak derivative* of a locally integrable function $u : \mathbb{R} \to \mathbb{C}$, if and only if

$$\int_{\mathbb{R}} v\, Du\, dx = -\int_{\mathbb{R}} u\, v' dx, \qquad \forall v \in C_0^1(\mathbb{R})$$

where $C_0^1(\mathbb{R})$ denotes continuously differentiable functions with compact support. We need the following well-known properties of weak derivatives:

1. Weak derivatives exist only for continuous functions (C^0).
2. A function has continuous weak derivative, if and only if it is continuously differentiable, i.e. C^1-function.

Remark 3.1 *We use the natural identification between continuous and locally integrable functions.*

By a week solution of (20) we understand a function satisfying

$$D(c\,Du) = -\omega^2 u \;\text{ on } \mathbb{R},$$

the equality holds in C^0-sense, i.e. pointwise. This is justified by the following considerations concerning a week solution u of (20):

1. Du must be defined, thus $u \in C^0(\mathbb{R})$.
2. $D(c\,Du)$ must be defined, thus $c\,Du \in C^0(\mathbb{R})$.
3. Since $D(c\,Du) = -\omega^2 u$ and $-\omega^2 u \in C^0(\mathbb{R})$, it follows by 1., that $D(c\,Du) \in C^0(\mathbb{R})$, hence $c\,Du$ must be in $C^1(\mathbb{R})$.

This allows us to search for a weak solution of (20) in the space

$$X_A := \{u \in C^0(\mathbb{R}) \,|\, c(x)\,Du(x) \in C^1(\mathbb{R})\} \subset C^0(\mathbb{R}).$$

Because of this we have the following corollary

Corollary 3.1 *Let $u : \mathbb{R} \to \mathbb{R}$ be a weak solution of (20). Then for all $x_0 \in \mathbb{R}$ it holds:*

$$u(x_0 + 0) = u(x_0 - 0); \tag{21a}$$
$$c\,Du\big|_{x=x_0+0} = c\,Du\big|_{x=x_0-0}. \tag{21b}$$

Remark 3.2 *If $x_0 \in G$, then the conditions (21) are called **interface conditions**. These conditions have the following physical interpretation: continuity of displacement and continuity of stress in material respectively.*

Now we are going to discover some properties of the weak solutions of (20). Since equation (20) is linear, it's solution space is also linear. We are interested in the dimension of the solution space, and for this we must find condition under which (20) has a unique solution. Let us recall a result from the theory of ordinary differential equations:

Proposition 3.1 *Let $A : (a,b) \to \mathbb{R}^{d\times d}$ be a bounded continuous function. Then the Cauchy problem*

$$u'(x) = A(x)\,u(x) \tag{22a}$$
$$u(a) = u_0 \tag{22b}$$

has a unique bounded solution for every $u_0 \in \mathbb{R}^d$, and the solution space of (22a) is a linear subspace of $C^0(\mathbb{R})$ with dimension d.

This helps to prove the following result:

Theorem 3.1 *Let $c \in C^1(\mathbb{R}\backslash G)$, where G is at most a countable set with no accumulation points. Assume $c'(x)$ is bounded in $\mathbb{R}\setminus G$. Then for every $x_0 \in \mathbb{R}\setminus G$ and $u_0, u_1 \in \mathbb{C}$, the Cauchy problem (20) with initial conditions $u(x_0) = u_0, u'(x_0) = u_1$ has a unique weak solution.*

Proof. Decompose $\mathbb{R}\setminus G$ into open intervals $\mathbb{R}\setminus G = \bigcup_{i\in I\subset\mathbb{Z}}$, so that $a_i{=}b_{i-1}$, and $x_0 \in (a_0, b_0)$. By Proposition 3.1, the Cauchy problem (20), $u(x_0) = u_0$, $u'(x_0) = u_1$ has a unique bounded solution in (a_0, b_0). The interface condition (21a) yields:

$$\begin{aligned} u(a_1+0) &= u(b_0-0); \\ u(b_{-1}-0) &= u(a_0+0); \end{aligned}$$

and (21b) yields

$$\begin{aligned} c(a_1+0)\,u'(a_1+0) &= c(b_0-0)\,u'(b_0-0); \\ c(b_{-1}-0)u'(b_{-1}-0) &= c(a_0+0)\,u'(a_0+0). \end{aligned}$$

From these conditions we obtain Cauchy data for (20) in (a_1, b_1) and (a_{-1}, b_{-1}). Proposition 3.1 guarantees existence and uniqueness of a bounded solution there.

By induction continuing the extension of the solution, we obtain the unique solution, as desired. ■

Corollary 3.2 *Under assumption of the above theorem the weak solution space of (20) is two-dimensional.*

3.2 Reduction to the one cell problem

In the classical analysis of periodic differential operators the Bloch-Floquet theorem is used to describe their spectrum. In its usual formulation (see [MAD]) it can be applied only to linear operators with *smooth* coefficients. Here we prove the theorem for more general function spaces, allowing it to be applied to (20).

3.2.1 Abstract Bloch-Floquet Theorem

First we need to introduce some notation. Let Z be a real finite dimensional linear vector space, and let $Y \subseteq \mathbb{C}^Z = \{\varphi : Z \longrightarrow \mathbb{C}\}$ be a *linear* function space.

For $p \in Z$, we define the *p-shift operator* $T_p : Y \to \mathbb{C}^Z$ by

$$T_p u(x) = u(x+p).$$

Let us assume that $T_p : Y \to Y$ is a bijection from Y to Y.[†]. Let $A : (X \subseteq Y) \to Y$ be a linear operator, where X is a linear space. The operator A is called *p-periodic* if and only if it commutes with T_p, i.e., $A \circ T_p = T_p \circ A$.

Given $\lambda \in \mathbb{C}$, the linear space

$$E_A(\lambda) = \{u \in X \;:\; Au = \lambda u\}$$

is called the *eigenspace* of A corresponding to the *eigenvalue* λ.

[†]Note that this does not hold for an arbitrary Y. For example it is not true for $Y = C^0(a,b)$, but is true for $Y = C^0(\mathbb{R})$

Theorem 3.2 (modified Bloch-Floquet) *Let $A : (X \subseteq Y) \to Y$ be a linear p-periodic operator, $p \neq 0$. Let $\lambda \in \mathbb{C}$ be such that $m := \dim E_A(\lambda) < \infty$.*

Then $E_A(\lambda)$ has a basis $\{\psi_1, \ldots, \psi_m\} \subset X$ with the property that

$$\forall k = 1, \ldots, m \quad \exists \gamma_k \in \mathbb{C} : T_p \psi_k(x) = \gamma_k \psi_k(x), \quad \forall x \in Z.$$

Proof. Suppose that $\varphi \in E_A(\lambda)$, i.e., $A\varphi = \lambda\varphi$. Then

$$AT_p\varphi = T_pA\varphi = T_p\lambda\varphi = \lambda T_p\varphi,$$

thus $T_p\varphi \in E_A(\lambda)$.

Choose a basis $\{\phi_1, \ldots \phi_m\}$ of $E_A(\lambda)$. Then for all $k = 1, \ldots, m$ holds: $T_p\phi_k \in E_A(\lambda)$. But since ϕ_k's form a basis, there exist complex numbers μ_j^k such that

$$T_p\phi_k = \sum_{j=1}^{m} \mu_j^k \phi_j.$$

The system $\{T_p\phi_1, \ldots, T_p\phi_m\}$ is linearly independent since the linear shift operator cannot destroy this property thus the matrix $M = (\mu_j^k)$ is nonsingular (here k is the row index and j is the column index).

Without loss of generality, we may assume that the matrix M is diagonalizable (if not, then we choose another basis for $E_A(\lambda)$ thus essentially performing elementary operations on the matrix).

Thus M possesses a complete set of eigenvectors $v^k = (v_1^k, \ldots, v_m^k)^T$ with

$$Mv^k = \gamma_k v^k, \qquad k = 1, \ldots, m. \tag{23}$$

Now define for $k = 1, \ldots m$

$$\psi_k = \sum_{j=1}^{m} v_j^k \phi_j.$$

We claim that $\{\psi_1, \ldots, \psi_m\}$ is the sought basis.

This system is a basis of $E_A(\lambda)$ by construction. It remains to show that $T_p\psi_k = \gamma_k\psi_k$:

$$\begin{aligned} T_p\psi_k &= T_p \sum_{j=1}^{m} v_j^k \phi_j = \sum_{j=1}^{m} v_j^k T_p \phi_j \\ &= \sum_{j=1}^{m} v_j^k \sum_{i=1}^{m} \mu_i^j \phi_i = \sum_{i=1}^{m} \phi_i \sum_{j=1}^{m} \mu_i^j v_j^k \\ &= \gamma_k \sum_{i=1}^{m} v_i^k \phi_i = \gamma_k \psi_k \end{aligned}$$

This completes the proof. ■

In what follows, we will refer to the basis from the theorem as *Bloch basis*, and functions that are described by a Bloch basis as *Bloch waves*.

3.2.2 Application

The abstract Bloch-Floquet theorem is a powerful tool to study (20). To apply it, we re-formulate (20) as an abstract eigenvalue problem.

Define the operator $A : X_A \to C^0(\mathbb{R})$ by

$$Au := D(c(x)Du(x)),$$

where D denotes the weak derivative. Then (20) can be written as an abstract eigenvalue problem:

$$A\,u = -\omega^2\,u.$$

Clearly, A is linear and p-periodic. Thus, the weak solution space of (20) coincides with the eigenspace $E_A(-\omega^2)$. We have already shown that
$\dim E_A(-\omega^2) = 2 < \infty$. Thus all the assumptions of the abstract Bloch-Floquet theorem are fulfilled, and the following Corollary follows:

Corollary 3.3 *For $\omega \in \mathbb{R}$, the space of weak solutions of (20) has a basis $\{\psi_1, \psi_2\}$ such that there exist $\gamma_1,\, \gamma_2 \in \mathbb{C}$ with*

$$T_p\psi_k = \gamma_k\psi_k, \quad k = 1, 2. \tag{24}$$

Remark 3.3 *Applying the Corollary n times we get*

$$T_{np}\psi_k = \psi_k(x + np) = \gamma_k^n\psi_k = e^{(\alpha_k + i\beta_k)n}\psi_k \qquad k = 1, 2.$$

Thus we see that the value of α_k can be interpreted as a damping (or amplification) from one cell to the next, whereas β_k corresponds to a phase shift from one cell to the next. If $\alpha_k = 0$, then the corresponding Bloch wave ψ_k passes through the filter undamped. Otherwise, if $\alpha_k < 0$ the Bloch wave is damped in the positive direction, and if $\alpha_k > 0$ it is damped in the negative direction‡.

If for some ω one of the Bloch waves is damped, then all solutions of (20) are also damped. Thus, we are interested in the behaviour only of the Bloch waves. So, let ω be fixed and ψ the corresponding Bloch wave. Using (24) we can derive a boundary value problem for ψ in a single cell. Direct application of (24) gives:

$$\psi(p+) = \gamma\,\psi(0+).$$

Because of (21a) this becomes:

$$\psi(p-) = \gamma\,\psi(0+). \tag{25}$$

Applying (24) for the weak derivative of ψ we obtain:

$$\psi'(p+) = \gamma\,\psi'(0+). \tag{26}$$

Because of (21b) we have:

$$c(p+)\psi'(p+) = c(p-)\,\psi'(p-). \tag{27}$$

Using the periodicity of c and substituting (27) into (26) we finally get:

$$c(p-)\,\psi'(p-) = \gamma\,c(0+)\,\psi'(0+). \tag{28}$$

‡We note that since the space domain for equation (20) is the whole real line, the output and input ends are not specified. Thus, whether $|u(x,\omega)| \xrightarrow[x\to+\infty]{} 0$ or $|u(x,\omega)| \xrightarrow[x\to-\infty]{} 0$ for fixed ω, we consider such waves damped.

Thus, instead of considering the Bloch wave ψ on the whole interval we may consider it only on one period, eg. $[0, p]$. Collecting (20), (25) and (28) we obtain the following boundary value problem for ψ:

$$\begin{cases} \dfrac{d}{dx}\left(c(x)\dfrac{d}{dx}\psi(x)\right) + \omega^2\psi(x) = 0 \\ \\ \psi(p) = \gamma\psi(0) \\ \\ c(p-)\,\psi'(p) = \gamma c(0+)\,\psi'(0) \end{cases} \tag{29}$$

which we will call ***the one cell problem***. In the following sections we will propose two different techniques to deal with (29).

4 Spectral Theory: Analytical Methods

Consider the one cell problem (29). **Let us fix ω from some interval, say $[0, 20]$. We are asking now: for which γ's does there exist nontrivial solutions of (29).** The solutions will have to be Bloch waves on $[0, p]$, and γ are multiplication factors in (24) (see Remark 3.3). If $\alpha := \ln|\gamma| = 0$, then the Bloch wave is a passing wave (since there is no damping) and the corresponding frequency ω is a passing frequency, otherwise not. In this section we derive an analytic technique to compute α, and thus the passing and damped frequency intervals.

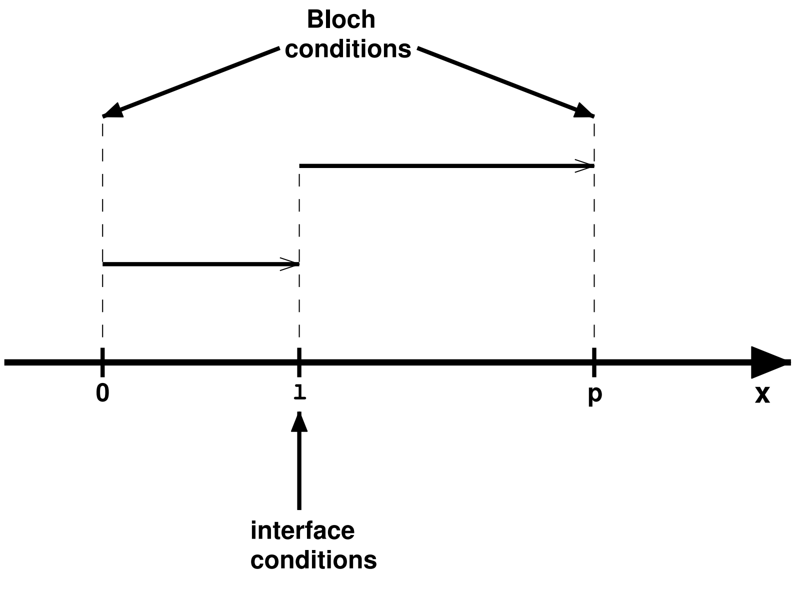

Figure 9: Chosen cell.

We choose a single cell as shown in Figure 9. In the continuity domains of $c(x)$, equation (20) becomes a simple ordinary differential equation with constant coefficients:

$$\begin{aligned} c_0\,\psi'' + \omega^2\,\psi = 0, &\quad x \in [0, l), \\ c_1\,\psi'' + \omega^2\,\psi = 0, &\quad x \in [l, p]. \end{aligned} \tag{30}$$

Solutions of (30) can be written analytically:

$$\psi(x) = \begin{cases} \psi_{(0)}(x) = a_{0,1} e^{i\frac{\omega}{\sqrt{c_0}}x} + a_{0,2} e^{-i\frac{\omega}{\sqrt{c_0}}x}, & x \in [0, l), \\ \psi_{(1)}(x) = a_{1,1} e^{i\frac{\omega}{\sqrt{c_1}}x} + a_{1,2} e^{-i\frac{\omega}{\sqrt{c_1}}x}, & x \in [l, p], \end{cases} \tag{31}$$

where $\{a_{i,j}\}$ are some constants.

At the interface $x = l$ we have the conditions (21a) and (21b), i.e.

$$\begin{aligned} \psi_{(0)}(l) &= \psi_{(1)}(l), \\ c_0 \psi'_{(0)}(l) &= c_1 \psi'_{(1)}(l). \end{aligned} \tag{32}$$

In the points $x = 0$ and $x = p$ we have the Bloch conditions:

$$\begin{aligned} \gamma \psi_{(0)}(0) &= \psi_{(1)}(p), \\ \gamma c_0 \psi'_{(0)}(0) &= c_1 \psi'_{(1)}(p). \end{aligned} \tag{33}$$

Substituting expressions (31) for $\psi_{(i)}$ into (32) and (33) we obtain a system of linear equations for the coefficients $\{a_{i,j}\}$. So let $\vec{a} = (a_{0,1}, a_{0,2}, a_{1,1}, a_{1,2})^\top$ and

$$M(\gamma, \omega) = \begin{pmatrix} e^{i\frac{\omega}{\sqrt{c_0}}l} & e^{-i\frac{\omega}{\sqrt{c_0}}l} & -e^{i\frac{\omega}{\sqrt{c_1}}l} & -e^{-i\frac{\omega}{\sqrt{c_1}}l} \\ c_0 i \frac{\omega}{\sqrt{c_0}} e^{i\frac{\omega}{\sqrt{c_0}}l} & -c_0 i \frac{\omega}{\sqrt{c_0}} e^{-i\frac{\omega}{\sqrt{c_0}}l} & -c_1 i \frac{\omega}{\sqrt{c_1}} e^{i\frac{\omega}{\sqrt{c_1}}l} & c_1 i \frac{\omega}{\sqrt{c_1}} e^{-i\frac{\omega}{\sqrt{c_1}}l} \\ \gamma & \gamma & -e^{i\frac{\omega}{\sqrt{c_1}}p} & -e^{-i\frac{\omega}{\sqrt{c_1}}p} \\ c_0 i \frac{\omega}{\sqrt{c_0}} \gamma & -c_0 i \frac{\omega}{\sqrt{c_0}} \gamma & -c_1 i \frac{\omega}{\sqrt{c_1}} e^{i\frac{\omega}{\sqrt{c_1}}p} & c_1 i \frac{\omega}{\sqrt{c_1}} e^{-i\frac{\omega}{\sqrt{c_1}}p} \end{pmatrix}$$

Then the system for coefficients $\{a_{i,j}\}$ has the following form:

$$M(\gamma, \omega)\, \vec{a} = \vec{0}. \tag{34}$$

We are only interested in the situation where (34) has nontrivial solution. This results in an equation for $\gamma(\omega)$:

$$\det\left(M(\gamma, \omega)\right) = 0. \tag{35}$$

Equation (35) is quadratic with respect to $\gamma(\omega)$ and can be solved analytically. As we have already mentioned, we are actually interested in the value of $\alpha = \ln|\gamma|$. The necessary computations were performed in Maple. All parameters were chosen as in Section 2. The computed results for $\alpha(\omega)$ are presented in Figure 10. Later they will be compared with the results obtained using the numerical technique derived in the next section.

5 Spectral Theory: Numerical Methods

The analytical method, presented in the previous section, strongly relies on the fact that equation (20) in the continuity domains of $c(x)$ could be solved analytically. That's why one may obtain analytical expression for the function from Bloch basis and for γ. This is because $c(x)$ was taken as a piecewise constant function (5). In general, when the function $c(x)$ is arbitrary (but periodic), analytical solutions are much more difficult to obtain. Moreover, in high dimensional models (2D or 3D) analytical solutions might be even harder to obtain, wherefor, one will have to rely on numerical techniques. Such a technique will be obtained here.

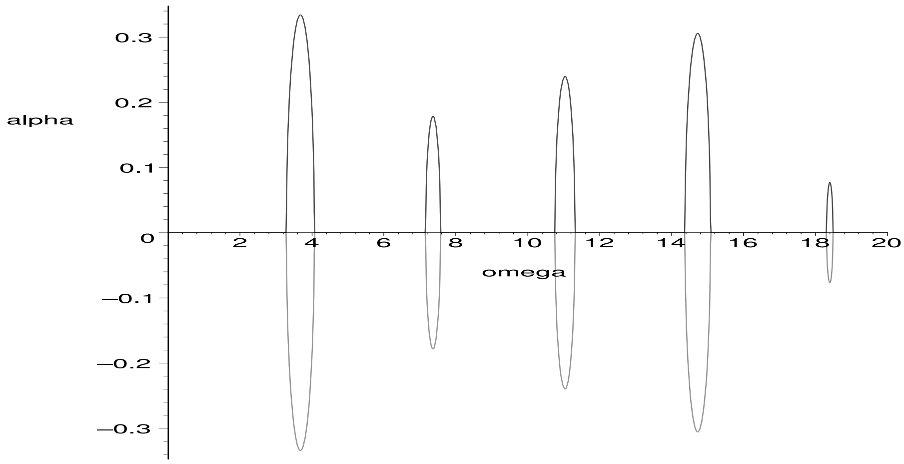

Figure 10: The values for α obtained using analytical technique. The intervals where $\alpha \neq 0$ correspond to the damped frequencies.

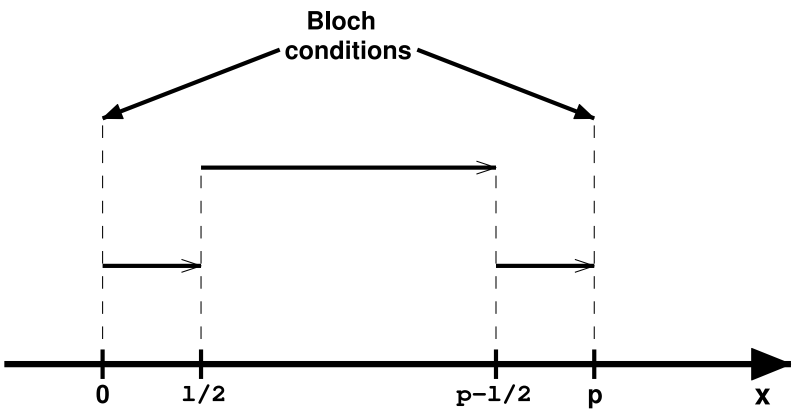

Figure 11: Chosen cell.

As in the previous section consider again (29). Instead of fixing ω and trying to find the corresponding γ, we are going to choose γ and then find corresponding ω's. We will look for undamped frequencies, that is $\gamma = e^{i\beta}$ with $\beta \in [0, 2\pi)$. So, let us fix some β. We are going to find ω for which (29) has non-trivial solution. We choose slightly different oriented cell (compared to the one in the last section) shown in Figure 11, so that the function $c(x)$ is continuous on the cell boundaries. Then the boundary conditions in (29) have the following form:

$$\psi(p) = e^{i\beta}\,\psi(0), \tag{36a}$$
$$\psi'(p) = e^{i\beta}\,\psi'(0). \tag{36b}$$

To design a numerical method, which approximates the solution of (29), we introduce an equidistant discretization of $[0, p]$:

$$x_i = \frac{p}{n-1}\,(i-1), \quad i = 1, ..., N.$$

Let us also denote

$$\begin{aligned} \boldsymbol{\psi_i} &= \psi(x_i), \\ x_{i+1/2} &= \frac{x_i + x_{i+1}}{2}, \\ h &= \frac{p}{N-1}. \end{aligned}$$

We will use the finite volume method to discretize (29):

$$\int\limits_{x_{i-1/2}}^{x_{i+1/2}} \frac{d}{dx}\left(c(x)\frac{d}{dx}\psi(x)\right) dx + \omega^2 \int\limits_{x_{i-1/2}}^{x_{i+1/2}} \psi(x)dx = 0.$$

By approximating $\frac{d}{dx}\psi(x_{i-1/2}) \approx \frac{\boldsymbol{\psi_i} - \boldsymbol{\psi_{i-1}}}{h}$ and $\int_{x_{i-1/2}}^{x_{i+1/2}} \psi(x)\,dx \approx \boldsymbol{\psi_i}\,h$ we get

$$\begin{aligned} 0 =&[-c(x_{i-1/2})]\,\boldsymbol{\psi_{i-1}} + \\ &[-\omega^2 h^2 + \big(c(x_{i+1/2}) + c(x_{i-1/2})\big)]\,\boldsymbol{\psi_i} + \\ &[-c(x_{i+1/2})]\,\boldsymbol{\psi_{i+1}}, \quad i = 2, \ldots, N-1. \end{aligned} \tag{37}$$

To use the boundary conditions (36) we perform the integrations $\int_{x_1}^{x_{1+1/2}}$ and $\int_{x_{N-1/2}}^{x_N}$. Using similar approximations as before we get:

$$-c(x_{1+1/2})\frac{\boldsymbol{\psi_2} - \boldsymbol{\psi_1}}{h} + c(x_1)\psi'(x_1) - \omega^2\frac{h}{2}\boldsymbol{\psi_1} = 0, \tag{38a}$$
$$-c(x_N)\psi'(x_N) + c(x_{N-1/2})\frac{\boldsymbol{\psi_N} - \boldsymbol{\psi_{N-1}}}{h} - \omega^2\frac{h}{2}\boldsymbol{\psi_N} = 0. \tag{38b}$$

Because of (36a) we have that $\boldsymbol{\psi_1}\,e^{i\beta} = \boldsymbol{\psi_N}$, therefore wherever we have $\boldsymbol{\psi_N}$ we substitute it by $\boldsymbol{\psi_1}\,e^{i\beta}$. The boundary condition (36b) leads to $e^{i\beta}c(x_1)\psi'(x_1) = c(x_N)\psi'(x_N)$, since $c(x)$ is periodic. Thus, multiplying (38a) by $e^{i\beta}$ and summing it with (38b) we get:

$$-c(x_{1+1/2})\frac{\boldsymbol{\psi_2}e^{i\beta} - \boldsymbol{\psi_1}e^{i\beta}}{h} + c(x_{N-1/2})\frac{\boldsymbol{\psi_1}e^{i\beta} - \boldsymbol{\psi_{N-1}}}{h} - \omega^2\,h\,e^{i\beta}\boldsymbol{\psi_1} = 0.$$

By collecting terms we simplify the previous equation to

$$
\begin{aligned}
0 =& [-\omega^2 h^2 + \left(c(x_{1+1/2}) + c(x_{N-1/2})\right)]\, \boldsymbol{\psi_1} + \\
& [-c(x_{1+1/2})]\, \boldsymbol{\psi_2} + \\
& [-c(x_{N-1/2}) e^{-i\beta}]\, \boldsymbol{\psi_{N-1}}.
\end{aligned}
\tag{39}
$$

Combining equations (37) and (39) we get a system of $(N-1)$ linear equations with $(N-1)$ unknowns:

$$A(\beta, \omega) \cdot \vec{\boldsymbol{\psi}} = \vec{0}, \tag{40}$$

where $\vec{\boldsymbol{\psi}} = (\boldsymbol{\psi_1}, \boldsymbol{\psi_2}, \ldots, \boldsymbol{\psi_{N-1}})^\top$ and $A(\beta, \omega)$ is the corresponding $(N-1) \times (N-1)$ matrix which depends on β and ω.

So, our task is to find the pairs (β, ω) for which equation (40) has a non-trivial solution. This is the same as to dertermine for which pairs, (β, ω), $\det A(\beta, \omega)$ is zero. An intuitive way to implement this numerically is to find the pairs for which $|\det A(\beta, \omega)| < \varepsilon$, for some small ε. But this leads to a very unstable algorithm with increasing discretization parameter N, and thus is useless. So, something else has to be tried.

Another idea is to change the problem (40) to an eigenvalue problem. We extract the terms with $-\omega^2 h^2$ from the left hand side of the equation (40) and move them to the right hand side. Then $\omega^2 h^2$ can be treated as an eigenvalue of the following problem:

$$C(\beta)\vec{\boldsymbol{\psi}} = \lambda \vec{\boldsymbol{\psi}} \tag{41}$$

with

$$\lambda = \omega^2 h^2$$

$$
C(\beta) = \begin{pmatrix}
* & * & & & & & * \\
* & * & * & & & & \\
& * & * & * & & & \\
& & \ddots & \ddots & \ddots & & \\
& & & * & * & * & \\
& & & & * & * & * \\
* & & & & & * & *
\end{pmatrix}
$$

where $*$ means a non-zero element and a blank means a zero element. To obtain eigenvalues of (41) one can use standard techniques.

The calculations are organized as follows:

- We choose N_β values of $\beta \in [0, 2\pi]$ as

$$\beta_i = \frac{i-1}{N-1} 2\pi, \ i = 1, ..., N_\beta.$$

- We choose the number of points, N, in the discretization of the space domain $[0, p]$.
- Then for each β_i we compute the eigenvalues $\{\lambda_j^i \,|\, i = 1, ..., N_\beta, \ j = 1, ..., N-1\}$ of (41), and thus the passing frequencies $\{\omega_j^i \,|\, i = 1, ..., N_\beta, \ j = 1, ..., N-1\}$.

Numerical results were obtained in MATLAB and are gathered in Figures 12-14. The eigenvalue problem (41) was solved by the function `eig`. All necessary parameters were chosen as in Section 4, so that we can compare the obtained results.

First, we show how the spectrum of the matrix $C(\beta)$ changes with increasing N. In Figure 12 all $\{\omega^i_j\}$ are shown for $N = 21, 51, 101$. In all cases we choose $N_\beta = 201$. One sees that with increasing N the range of ω also increases. But if we denote $\{\omega^i_{(j)}\}$ the j-th smallest value of $\omega^i_\cdot$, then there should exist a limit $\lim\limits_{N\to\infty} \omega^i_{(j)}$. In Figure 13 the first 5 smallest $\omega^i_\cdot$ are shown. In this case we have chosen $N = 101$. The mentioned convergence has been observed numerically. So, this picture is barely changed after $N = 51$. Thus, with increasing N the values of ω are allocating in some intervals. One can see in Figure 13 that there are intervals which do not contain any $\{\omega^i_j\}$, therefore these intervals correspond to the damped frequencies (these intervals cannot be seen in Figure 12 due to scaling).

Finally, in Figure 14 damped frequency intervals obtained by numerical and analytical techniques are compared. Here we choose $N = 201$ for numerical method. One can see that damped frequency intervals fit together.

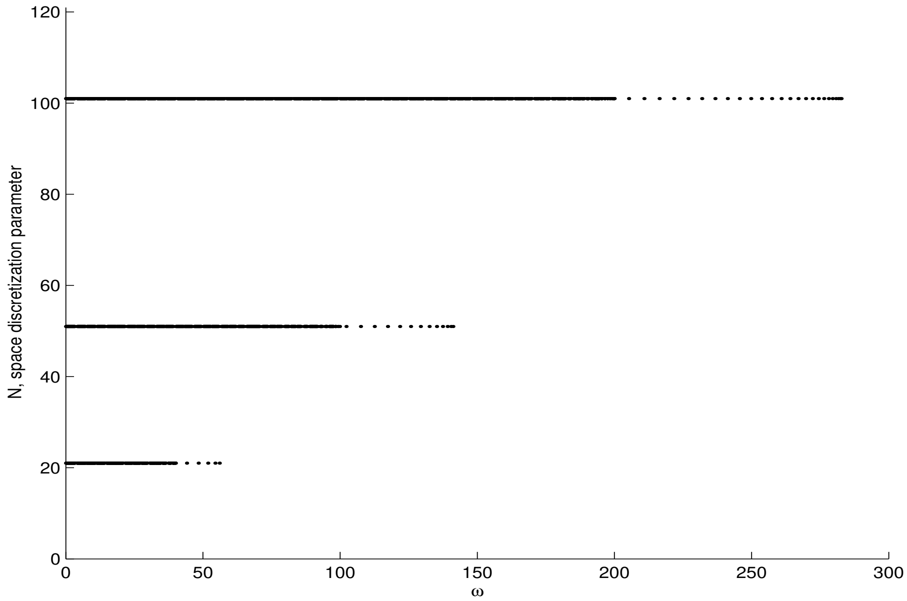

Figure 12: The values of all $\{\omega^i_j\}$ obtained for $N = 21, 51, 101$.

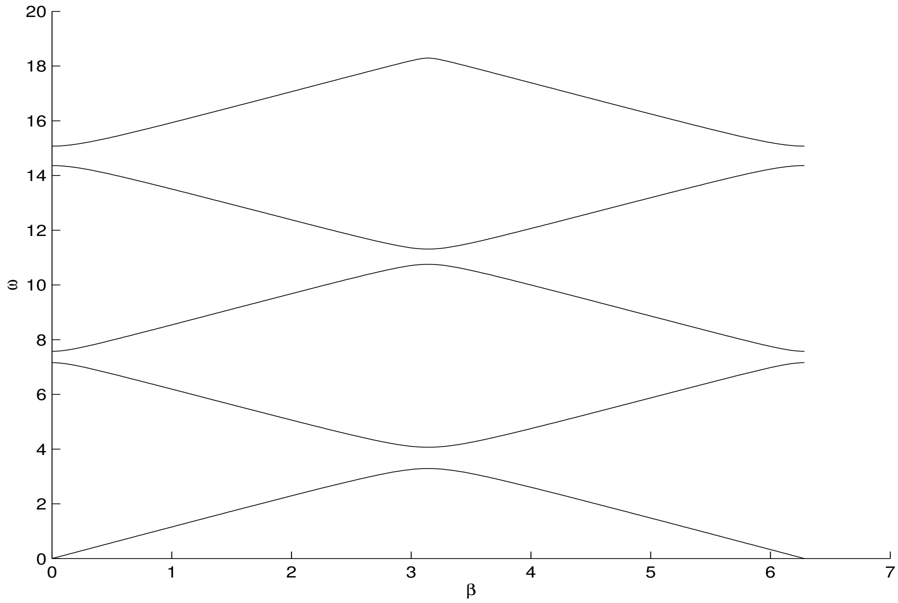

Figure 13: First 5 values of $\{\omega^i_{(j)}\}$ which correspond to the first 5 smallest eigenvalues of (41). $N = 101$.

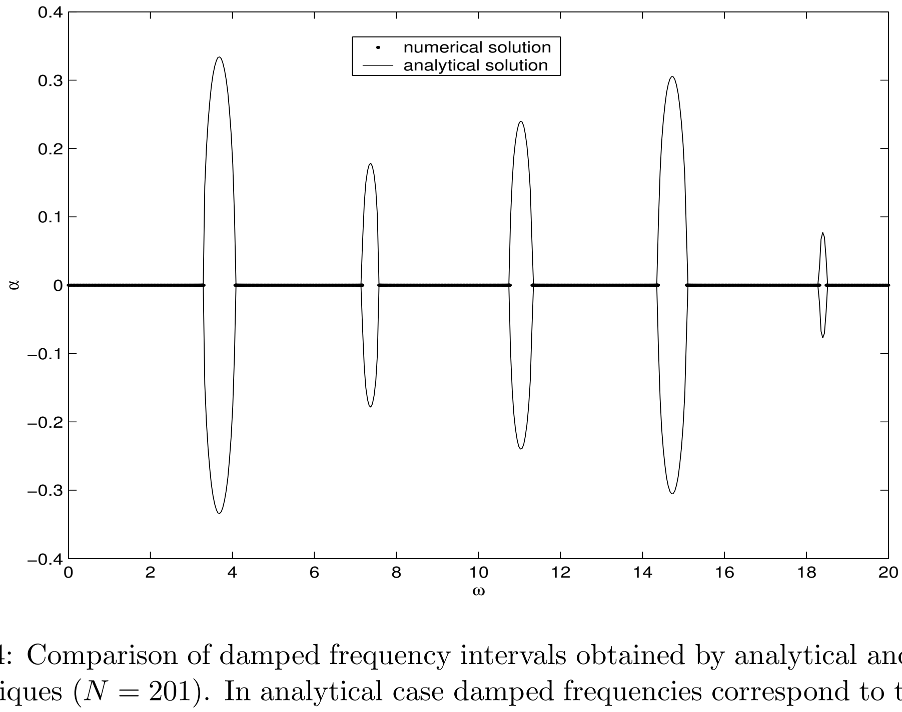

Figure 14: Comparison of damped frequency intervals obtained by analytical and numerical techniques ($N = 201$). In analytical case damped frequencies correspond to the values of $\alpha \neq 0$. Numerical method always gives frequencies for $\alpha = 0$, i.e. undamped.

6 Summary and Outlook

The problem of computing passing/damped frequency intervals has been analyzed and different procedures were proposed for their calculations.

We first derived a 1D model for a filter consisting of small amount of cells. The developed numerical method provides a good demonstration of passing and damped frequencies. Unfortunately this numerical method cannot be applied to analyze the real filter, which consists of the huge amount of cells. Thus the model, which assumes that the filter occupies infinite domain, was obtained.

After shifting to the frequency domain we found a differential equation with periodic coefficients. For its analysis we stated and proved Bloch-Floquet Theorem, which allowed us to consider the problem in one cell instead on the whole real line. Two different approaches to the application of the theorem were proposed: analytical and numerical.

The analytical method was very fast and gave exact results, however it can only be applied for filters with a piecewise constant stiffness tensor c. The numerical methods on the other hand can be applied to arbitrary configurations. For the simple configuration considered in this paper, the results of the analytical and the numerical methods agreed, as would be expected.

Further work can be concentrated in the following directions:

- Extensive test of the proposed algorithms should be performed for different filter configurations (different materials, different periodicity).
- Design of higher dimensional models (2D and 3D) and their analysis is of interest.
- Finally, models which includes the piezoelectric coupling in equations (2a) and (2b) should be developed. Obtained results should be compared with experimental data.

References

[OLI] A.A.Oliner (editor), *Acoustic Surface Waves*, Springer, 1978.

[MCL] Peter McLean, *Signals and Systems*, Lecture Notes, World Wide Web, `http://www.eng.uts.edu.au/~pmclean/ss/Downloads/LectureNotes.pdf`, 2003.

[AUL] B.A.Auld, *Acoustic fields and waves in solids*, Wiley, 1973.

[MAD] O.Madelung, *Grundlagen der Halbleiterphysik*, Springer, 1970.

[TSM] A.N.Tychonoff and A.A.Samarski, *Differentialgleichungen der Mathematischen Physik*, VED Deutscher Verlag der Wissenschaften, Berlin, 1959.

[AMS] William F. Ames, *Numerical Methods for Partial Differential Equations*, Thomas Nelson and Sons LTD, 1969.